

## Supporting Information

### **PCL Microspheres Tailored with Carboxylated Poly(glycidyl methacrylate)-REDV Conjugates as Conductive Microcarriers for Endothelial Cell Expansion**

Shaojun Yuan,<sup>a,#,\*</sup> Gordon Xiong,<sup>b,#</sup> Fei He,<sup>a</sup> Wei Jiang,<sup>a</sup> Bin Liang,<sup>a</sup> Cleo Choong<sup>b,\*</sup>

<sup>a</sup>Multiphase Mass Transfer & Reaction Engineering Lab,  
College of Chemical Engineering,  
Sichuan University, Chengdu, China, 610065

<sup>b</sup>School of Materials Science and Engineering,  
Nanyang Technological University,  
50 Nanyang Avenue, Singapore 639798

---

# These authors contributed equally.

\*To whom all correspondence should be addressed

Tel: +86-28-85990133, Fax: +86-28-85460556

E-mail: [yuanshaojun@gmail.com](mailto:yuanshaojun@gmail.com) (S.J. Yuan), [cleochoong@ntu.edu.sg](mailto:cleochoong@ntu.edu.sg) (C. Choong)

## Results and Discussion

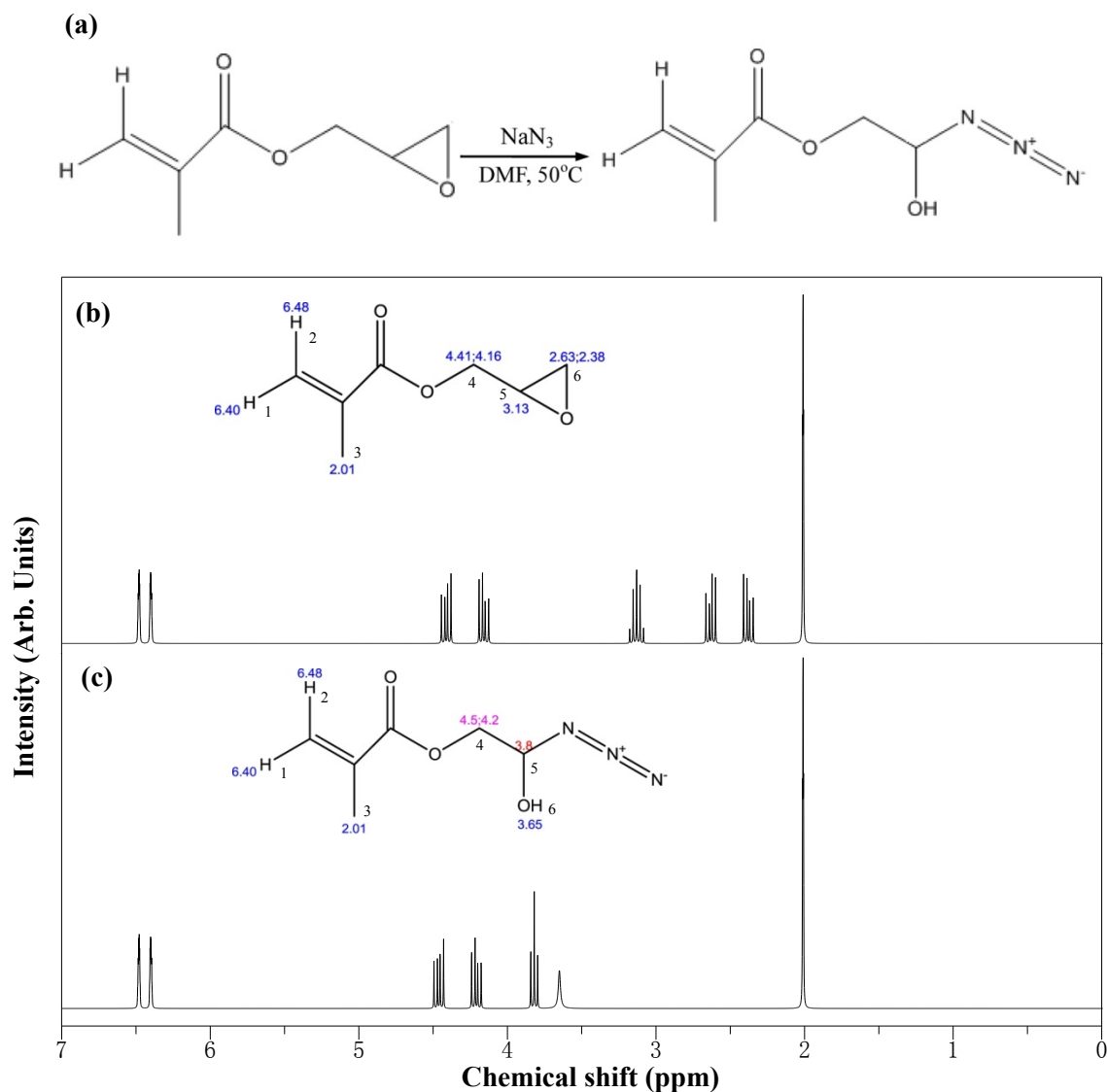


**Fig. S1** (a) The synthesis route of azide-terminated GMA-N<sub>3</sub> monomer, (b,c) <sup>1</sup>H NMR spectra comparison of GMA and GMA-N<sub>3</sub> monomers in CDCl<sub>3</sub> solvent. Successful synthesis of GMA-N<sub>3</sub> monomer can be deduced from the disappearance of methylene protons in 2.38 and 2.63 ppm and methyl hydrogen in 3.13 ppm for the epoxy ring and the appearance of hydroxyl proton in 3.65 ppm and methyl hydrogen in 3.8 ppm.

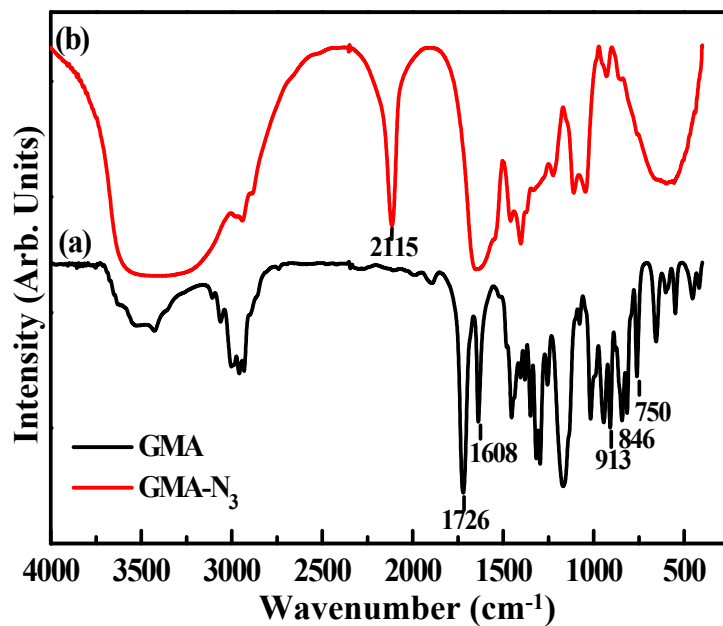


**Fig. S2** FTIR spectra of the (a) GMA and (b) as-synthesized GMA-N<sub>3</sub> monomers. Successful synthesis of GMA-N<sub>3</sub> monomer was ascertained by the disappearance of the characteristic epoxide bands with wavenumbers at 750, 846 and 913 cm<sup>-1</sup> and the appearance of additional peak of azide stretching vibration ( $\nu_{N_3}$ ) at 2115 cm<sup>-1</sup>.

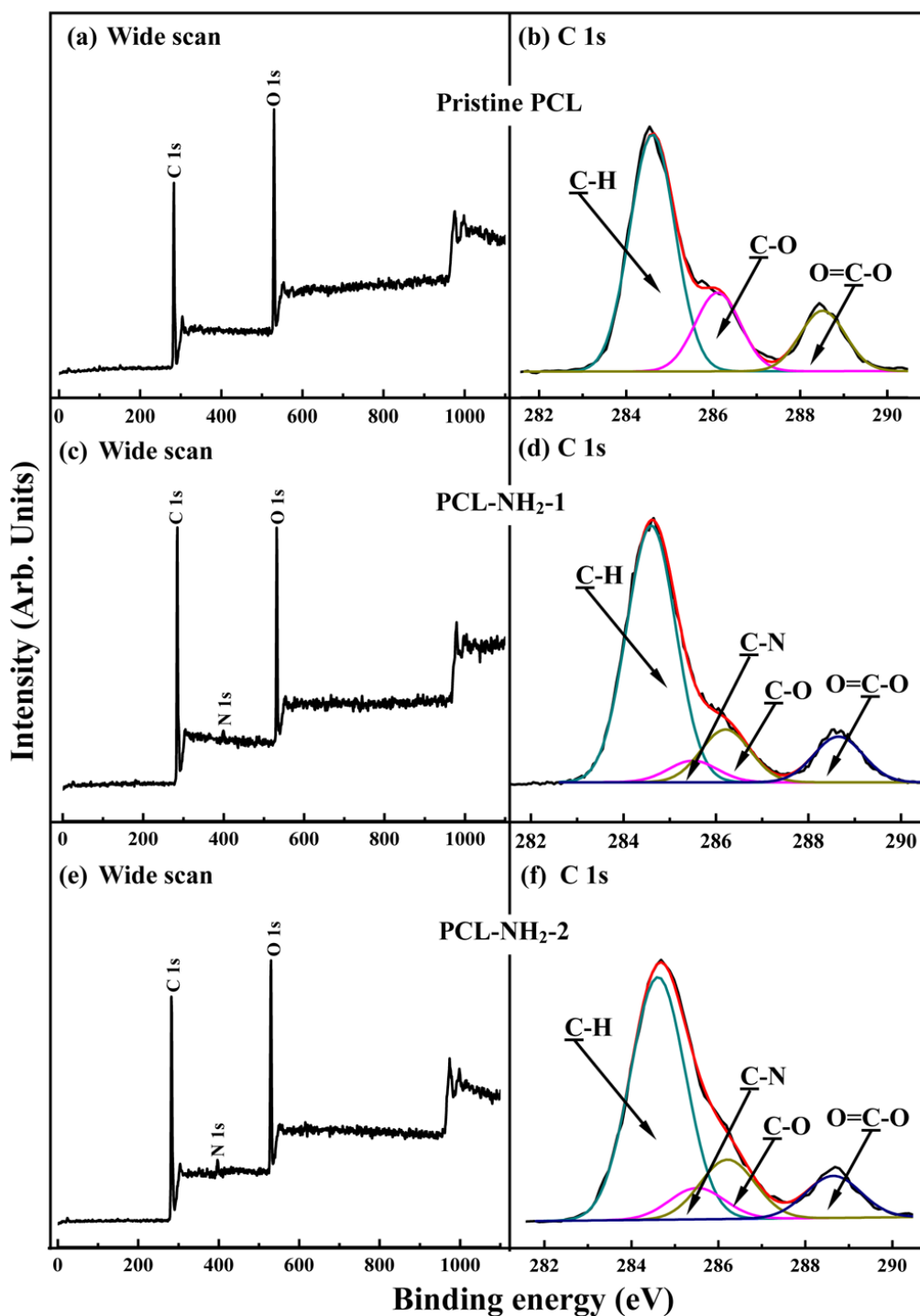


**Fig. S3** Wide scan and C 1s core-level XPS spectra of the (a,b) pristine PCL, (c,d) PCL-NH<sub>2</sub>-1 (from 30 min of aminolysis) and (e,f) PCL-NH<sub>2</sub>-2 (from 60 min of aminolysis). The appearance of additional N 1s signals indicated the successful introduction of amino groups on the PCL substrates.

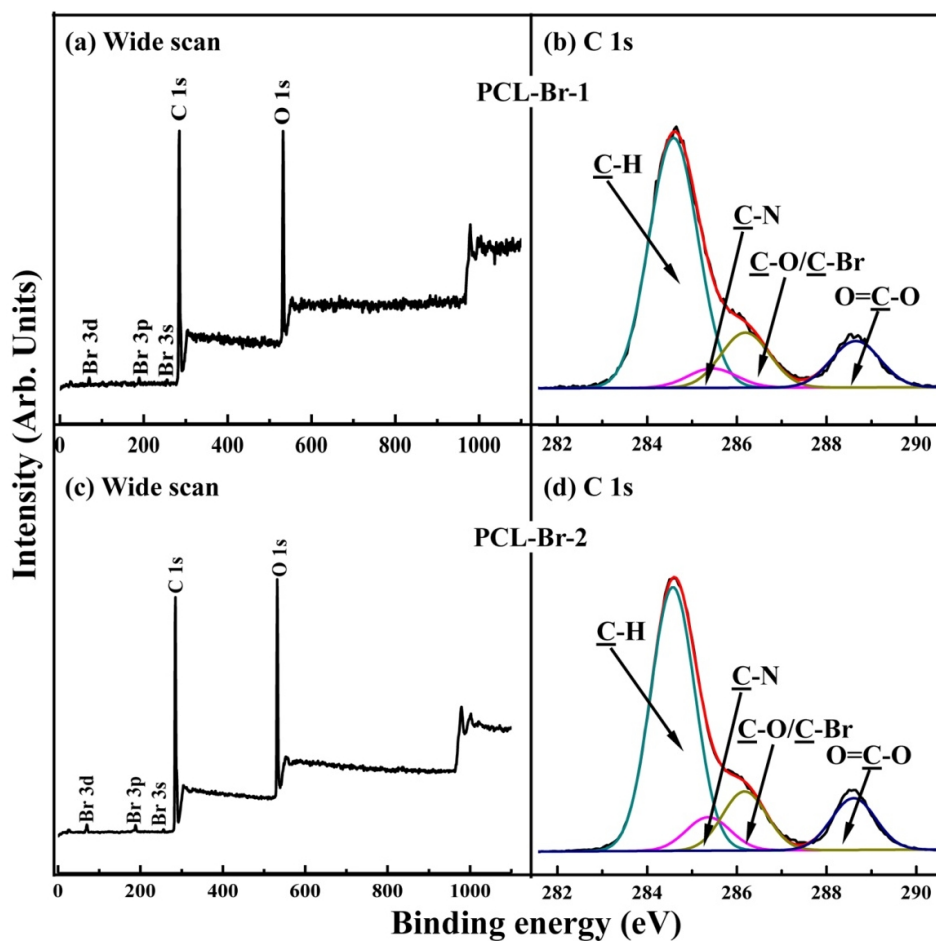


**Fig. S4** Wide scan and C 1s core-level XPS spectra of the (a,b) PCL-Br-1 (from PCL-NH<sub>2</sub>-1 surface) and (c,d) PCL-Br-2 (from PCL-NH<sub>2</sub>-2 surface). The appearance of additional Br 3d, Br 3p and Br 3s signals indicated the successful introduction of an alkyl bromide-terminated ATRP initiator.

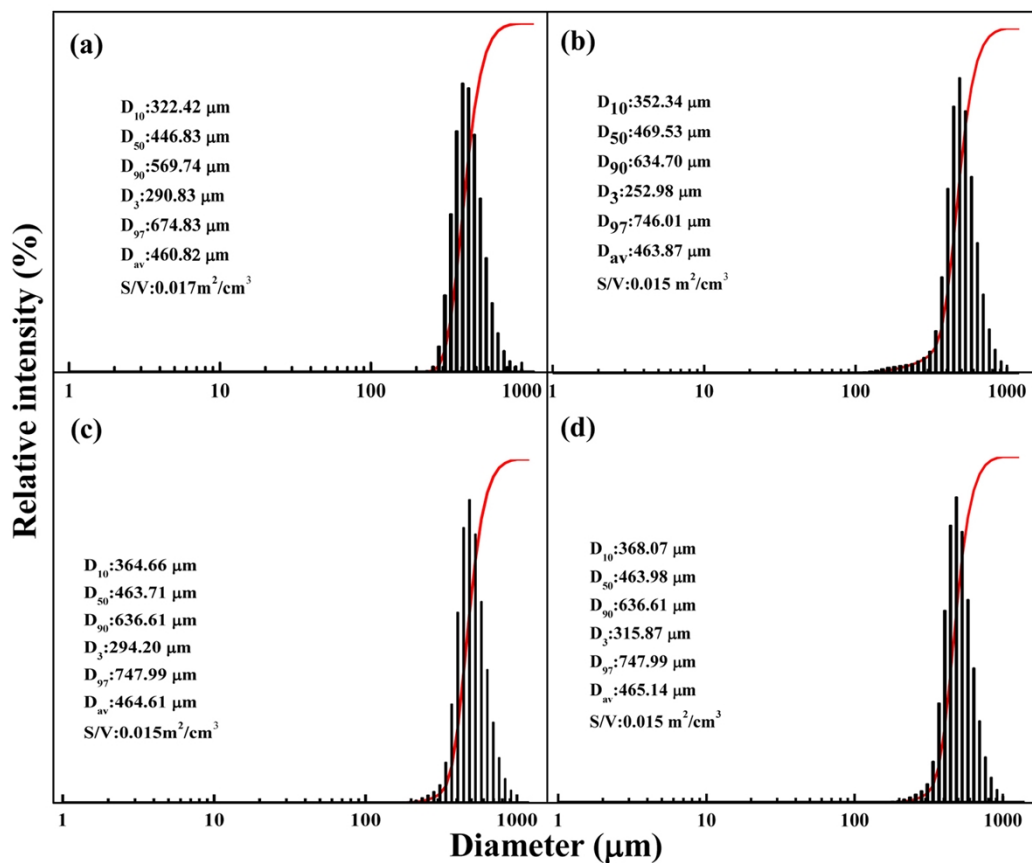


**Fig. S5** Size distribution curves to illustrate the size distribution of the (a) PCL-g-PGMA1-N<sub>3</sub>, (b) PCL-g-PGMA2-N<sub>3</sub>, (c) PCL-g-PCGMA2-COOH, and (d) PCL-g-CPGMA2-c-REDV microspheres. The change in average diameters was indicative of successful functionalization of PCL microspheres.

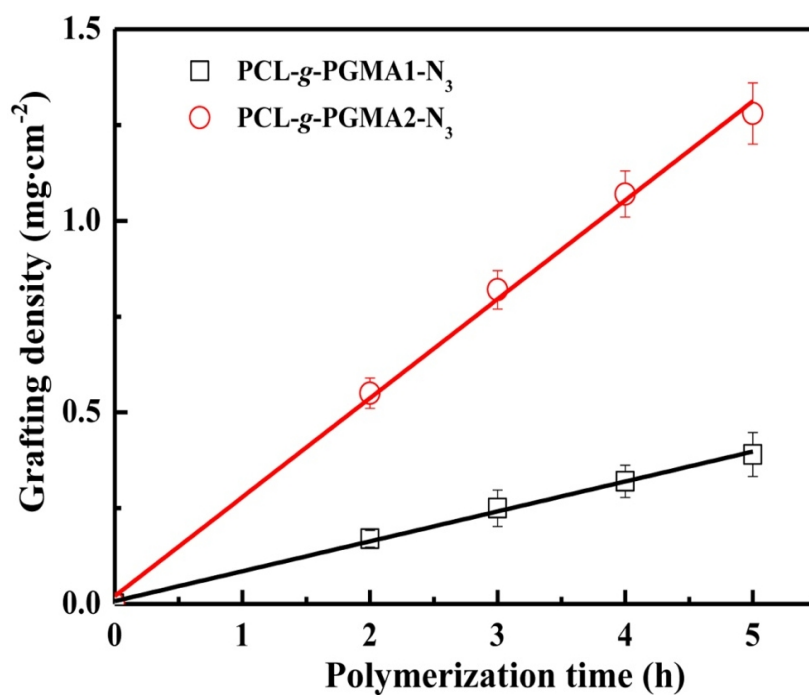


**Fig. S6** A linear increase in the grafting density of the PGMA-N<sub>3</sub> brushes via surface-initiated ATRP from the PCL-Br-1 (black line) and PCL-Br-2 (red line) surfaces as a function of reaction time. The PGMA-N<sub>3</sub> chain growth on the PCL substrates was found to proceed in a well-controlled manner by varying the surface density of ATRP initiator and reaction time.

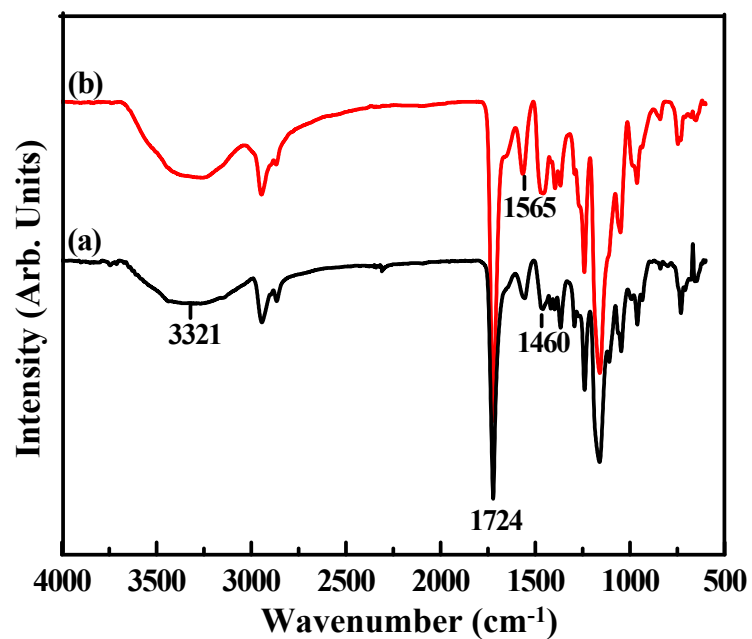


**Fig. S7** ATR-FTIR spectra of the surfaces of the (a) PCL-g-CPGMA1-COOH and (b) PCL-g-GMA2-COOH microspheres. Successful carboxylation of PGMA-N<sub>3</sub> brushes was verified by the disappearance of characteristic bands with wavenumber at about 2106 cm<sup>-1</sup> and the appearance of a broad band at wavenumber of 3600-3200 cm<sup>-1</sup>, attributable to H-bonded O-H stretching vibration.